Biol Trace Elem Res
DOI 10.1007/s12011-015-0331-6

Tungsten Carbide-Cobalt Nanoparticles Induce Reactive Oxygen Species, AKT, ERK, AP-1, NF-κB, VEGF, and Angiogenesis

Ling-Zhi Liu[1] · Min Ding[2] · Jenny Z. Zheng[3] · Yingxue Zhu[1] · Bruce A. Fenderson[1] · Bingyun Li[4] · Jing J. Yu[3] · Bing-Hua Jiang[1]

Received: 21 January 2015 / Accepted: 6 April 2015

Abstract Powder mixtures of tungsten carbide and metallic cobalt (WC-Co) are widely used in various products. Nanoparticles are engineered structures with at least one dimension of 100 nm or smaller. WC-Co is known to be associated with lung injury and diseases. Angiogenesis is a key process during vasculature, carcinogenesis, recovery of injury, and inflammatory diseases. However, the cellular effects of WC-Co nanoparticles on angiogenesis remain to be elucidated. In this study, we investigated angiogenic response and relative mechanisms after exposure to WC-Co nanoparticles. Our results showed that WC-Co nanoparticles at 5 μg/cm^2 induced ROS production which activated AKT and ERK1/2 signaling pathways in lung epithelial cells by reactive oxygen species (ROS) staining and immunoblotting; WC-Co treatment also increased transcriptional activation of AP-1, NF-κB, and VEGF by reporter assay. Further studies demonstrated that ROS are upstream molecules of AKT and ERK signaling pathways; the activation of AP-1, NF-κB, and VEGF was through ROS generation, AKT and ERK1/2 activation. In addition, WC-Co nanoparticles affected the cells to induce angiogenesis by chicken chorioallantoic membrane (CAM) assay. These results illustrate that exposure to WC-Co nanoparticles induces angiogenic response by activating ROS, AKT, and ERK1/2 signaling pathways and the downstream molecules and elucidate the potential molecular mechanisms during this process. This information may be useful for preventing potential damage from nanoparticle exposure in the future.

Keywords Carbide-cobalt nanoparticles · Reactive oxygen species · Signaling pathways · VEGF · Angiogenesis

Abbreviations

WC-Co	Tungsten carbide and metallic cobalt
ROS	Reactive oxygen species
CAM	Chicken chorioallantoic membrane
PBS	Phosphate-buffered saline
DCFH-DA	2′,7′-Dichlorofluorescein diacetate
H_2O_2	Hydrogen peroxide
AP-1	Activator protein-1
NF-κB	Nuclear factor kappa B
VEGF	Vascular endothelial growth factor
ERK	Extracellular signal regulated kinase

Introduction

Nanotechnology is one of the fastest growing emerging technologies and has a wide range of applications such as integrated sensors, semiconductors, medical imaging, drug delivery, structural materials, sunscreens, cosmetics, and coatings [1]. Nanoparticles have at least one dimension of 100 nm or smaller. This small size results in properties which may

✉ Ling-Zhi Liu
ling-zhi.liu@jefferson.edu

✉ Bing-Hua Jiang
bhjiang@jefferson.edu

[1] Department of Pathology, Anatomy and Cell Biology, Thomas Jefferson University, Philadelphia, PA, USA

[2] Health Effects Laboratory Division, National Institute for Occupational Safety and Health, Morgantown, WV, USA

[3] Mary Babb Randolph Cancer Center, Department of Biochemistry, West Virginia University, Morgantown, WV, USA

[4] Department of Orthopedics, West Virginia University, Morgantown, WV, USA

Published online: 19 April 2015

substantially differ from particles of the same composition in the micrometer scale. Intensive researches focused on the development of nanotechnology could lead to an increasing risk of exposure to nanoparticles over the next few years. There are increasing public concerns over the adverse health effects of exposure to nanoparticles and possible environmental impact of this emerging nanotechnology. Recent evidence has indicated that nanoparticles exhibit a higher deposition in all regions of the respiratory tract when compared to the fine particles, and that exposure to nanoparticles may induce cytotoxicity, pulmonary inflammation, and/or other adverse effects in the cells and the lung [2–5]. Once deposited in the airways, nanoparticles may migrate more rapidly to the interstitium and lymph nodes of the lung than the fine particles [6]. However, the mechanisms involved in potential bioactivity of nanoparticles leading to the adverse effects are poorly understood.

Hard metal or cemented carbide consists of a powder mixture by 80 to 90 % of tungsten carbide (WC) and 5 to 10 % of metallic cobalt (Co). It has been demonstrated that the inhalation of hard metal particles may cause an interstitial pulmonary disease and lung cancer, the mechanism of which involves an interaction between Co and WC particles, the generation of reactive oxygen species, and oxidant-induced DNA-damage [7–12]. WC-Co exposure leads to hard metal pulmonary disease, giant cell interstitial pneumonia, and lung fibrosis [13–15], and may be related with lung carcinoma [16]. A recent study indicates that WC-Co particles in the nano-size range can be internalized by lung epithelial cells, suggesting that internalization may play a key role in the enhanced toxicity of nano-WC-Co particles over micro-WC-Co particles [17]. However, the effect of WC-Co on angiogenesis response remains to be elucidated. In this study, we analyze the effects of WC-Co nanoparticles in regulating the production of reactive oxygen species (ROS), the transcriptional activation of AP-1, NF-κB, and VEGF, the activation of AKT or extracellular signal regulated kinase (ERK), and the induction of angiogenesis.

Materials and Methods

Cell Culture

BEAS-2B, the normalized human bronchial epithelial cells from the lungs, were cultured in DMEM supplemented with 10 % FBS and 100 units/ml penicillin and 100 μg/ml streptomycin and cultured at 37 °C in a 5 % CO_2 incubator. Human lung adenocarcinoma cells A549 were cultured in RPMI 1640 supplemented with 10 % FBS and antibiotics under the same condition.

Adenovirus

The construction of dominant-negative AKT (AKT-K179M) and GFP has been described previously [18]. Recombinant adenoviruses were made using the AdEasy system [19]. Viral titers were determined using the BD Adeno-X™ Rapid Titer Kit (BD Biosciences Clontech, Mountain View, CA) according to the user manual.

Angiogenesis Using the CAM Assay

Fertilized white Leghorn chicken eggs were incubated at 37 °C with 70 % humidity for 9 days. An artificial air sac was created over a region containing small blood vessels in the chicken chorioallantoic membrane (CAM) as described [18]. To test angiogenesis, the cells were suspended in serum-free medium containing 50 % Matrigel (BD Biosciences, Bedford, MA). Aliquots (3×10^6 cells, 30 μl) of the mixture were then applied onto the CAM of 9-day-old embryos. The area around the implanted Matrigel was photographed 4 days after the implantation, and the number of blood vessels was obtained by counting the branching of blood vessels. The experiments were performed using 8~10 chicken embryos for each treatment.

Intracellular Hydrogen Peroxide (H_2O_2) Detection

BEAS-2B cells were seeded on coverslips in a 6-well plate and cultured overnight. After treated without (the control) or with 5 μg/cm^2 fine- or nano-sized WC-Co for the indicated period time, the cells were incubated with 5 μM 2′,7′-dichlorofluorescein diacetate (DCFH-DA) for 15 min. The cells were washed twice with phosphate-buffered saline (PBS) and fixed with 10 % buffered formalin for 10 min. DCFH-DA diffuses through the cell membrane and is rapidly oxidized to highly fluorescent dichlorofluorescein in the presence of H_2O_2. The fluorescent images were captured using a fluorescence microscope. For the treatments with catalase, LY294002, or U0126, cells were pretreated with these reagents for 30 min. Then, the particles were added, and cells were treated as above.

Transient Transfection and Luciferase Assay

BEAS-2B cells were seeded in 12-well plates and cultured to 70 % confluence. The cells were transiently transfected with activator protein-1 (AP-1), nuclear factor kappa B (NF-κB), or vascular endothelial growth factor (VEGF) reporter plasmids and pCMV-β-galactosidase (β-gal) using Lipofectamine (Invitrogen, Carlsbad, CA) according to the manufacturer's instructions. After transfection,

the cells were cultured overnight, followed by different treatments. Cells were then washed and lysed with reporter lysis buffer (Promega, Madison, WI). The luciferase (Luc) activities of the cell extracts were determined using the luciferase assay system (Promega, Madison, WI). The relative luciferase activity (defined as reporter activity) was calculated as the ratio of Luc/β-gal activity and normalized to the control.

Western Blotting

The cells were lysed in RIPA buffer supplemented with DTT and proteinase inhibitors. The cellular lysates were clarified by centrifugation at 15,000×*g* for 10 min. Aliquots of the protein extracts were resolved in SDS/polyacrylamide gels and transferred to nitrocellulose membranes. Membranes were blocked with 5 % nonfat dry milk in 1× PBS buffer containing 0.05 % Tween 20 and incubated with antibodies against phospho-AKT, total AKT, phospho-ERK1/2 (Cell Signaling Technology, Beverly, MA), and total ERK2 (Santa Cruz Biotechnology, Santa Cruz, CA). Specific protein signals were detected by incubating with horseradish peroxidase-conjugated antibodies and visualizing with a chemiluminescence reagent (Pierce Biotechnology, Rockford, IL).

Statistical Analysis

The data represent mean±SD from three independent experiments except where indicated. Statistical analysis was performed by Student *t* test at a significant level ($p<0.05$).

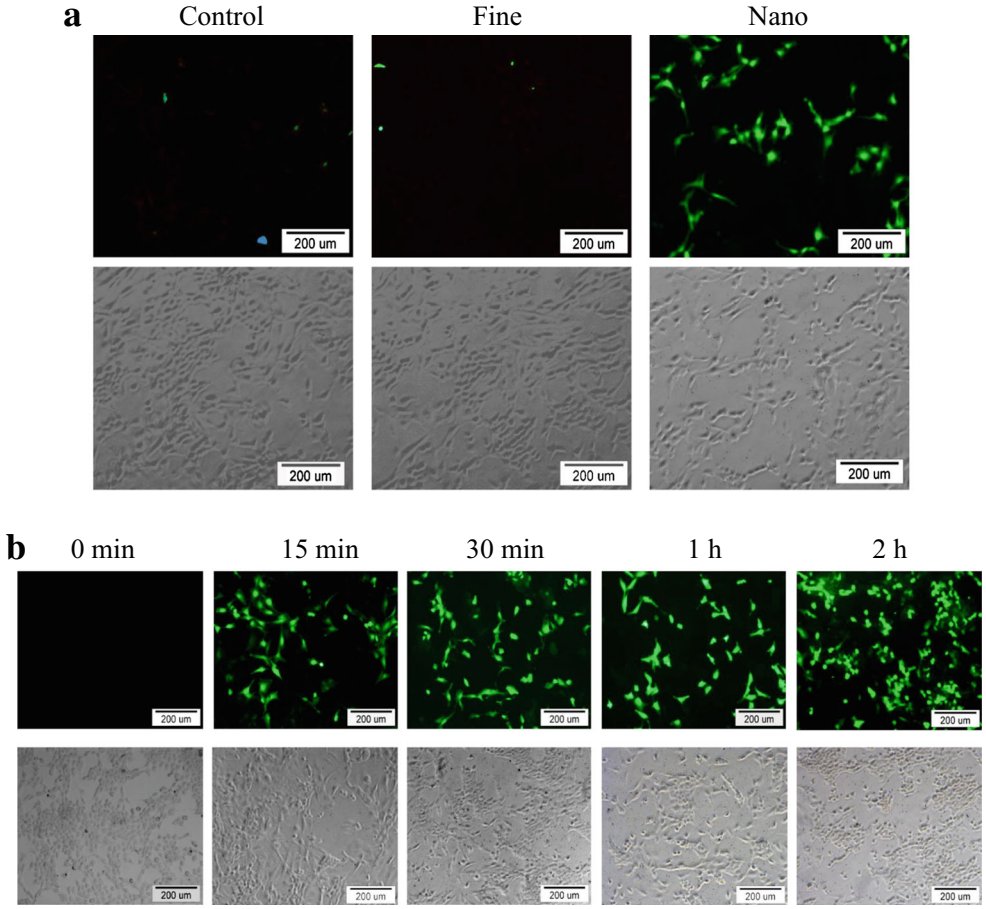

Fig. 1 Nano-sized tungsten carbide-cobalt (WC-Co) increased ROS production. **a** BEAS-2B cells were seeded onto coverslips in 6-well plate and incubated at 37 °C for 24 h. The cells were cultured in fresh serum-free medium with fine-sized or nano-sized WC-Co at 5 μg/cm^2 for 30 min. DCFH-DA (5 μM) was added and incubated for 15 min. Then, the cells were washed and fixed. The images were captured with a fluorescence microscope (*upper panel*). The corresponding bright field micrographs are shown in the *bottom panel*. *Bar*: 200 μm. **b** BEAS-2B cells were seeded onto a glass slip in the 6-well plate and incubated at 37 °C for 24 h. The cells were then cultured in serum-free medium with nano-size of WC-Co at 5 μg/cm^2 for the time as indicated. DCFH-DA (5 μM) was added and incubated with the cells for 15 min. Then, the cells were washed and fixed, and the images were captured as above. The fluorescent images were captured using a confocal fluorescence microscope (*upper panel*). The corresponding micrographs are shown in the *bottom panel*. *Bar*: 200 μm

Results

WC-Co Nanoparticles Induced Reactive Oxygen Species (ROS) Production

ROS include superoxide, hydrogen peroxide (H_2O_2), and hydroxyl radical. ROS have been demonstrated to be involved in regulating cell metabolism, apoptosis, proliferation, tumor angiogenesis, and progression, and are also secondary messengers [20–22]. To study whether nanoparticles of WC-Co can stimulate ROS generation, BEAS-2B cells were seeded on the coverslips, and cultured overnight, then treated with solvent, fine particles, or nano particles. The production of ROS was detected by DCFH-DA staining as previously described [23, 24]. The nano-sized WC-Co at 5 μg/cm^2 induced high levels of ROS production in the cells, while the treatment of cells with the solvent or the fine size WC-Co at 5 μg/cm^2 did not increase ROS generation (Fig. 1A). The ROS production was observed 15 min after WC-Co nanoparticle treatment and gradually increased up to 2 h (Fig. 1B). These results indicated that WC-Co nanoparticles at 5 μg/cm^2 strongly induced ROS production in BEAS-2B cells.

WC-Co Nanoparticles Induced AP-1, NF-κB, and VEGF Transcriptional Activation

AP-1 and NF-κB are important transcription factors related to pulmonary injury, inflammatory lesions, and angiogenesis. It has been reported that AP-1 and NF-κB is activated by hydrogen peroxide in various cell types [25, 26]. VEGF plays a key role in angiogenesis. Our previous studies have showed that ROS generation induced VEGF expression in ovarian and prostate cancer cells [23, 27]. To test whether WC-Co nanoparticles induced AP-1, NF-κB, and VEGF transcriptional activation, BEAS-2B cells were transfected with AP-1, NF-κB, or VEGF reporter plasmid with β-gal plasmid, then treated with nano- or fine-sized WC-Co particles. As shown in Fig. 2a–c, nano-sized WC-Co at 2.5 and 5 μg/cm^2 significantly induced AP-1, NF-κB, and VEGF transcriptional activation, while fine-sized WC-Co did not significantly affect their transcriptional activation at those doses.

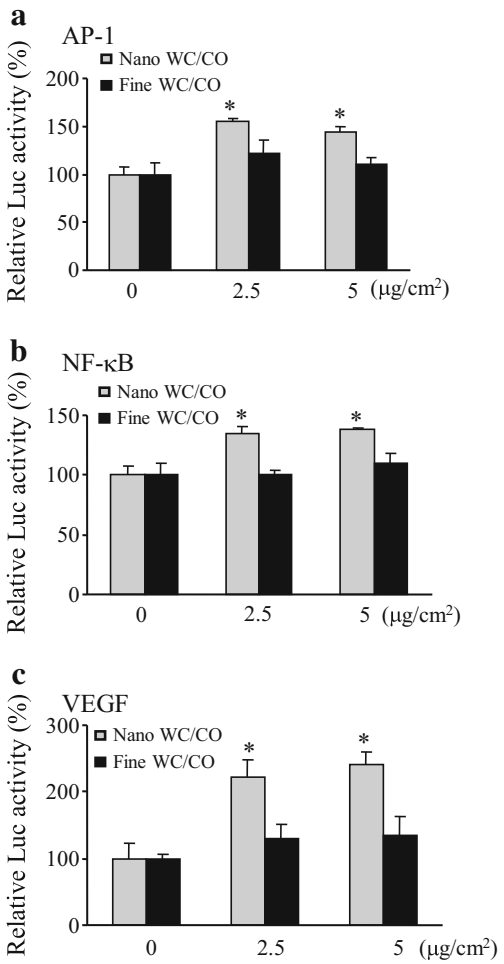

Fig. 2 WC-Co nanoparticles induced AP-1, NF-κB, and VEGF transcriptional activation. **a** Cells were co-transfected with β-gal plasmid (0.2 μg) and AP-1 reporter plasmid (0.4 μg). After transfection, the cells were cultured overnight in fresh medium, then treated with nano or fine size WC-Co (0, 2.5, and 5 μg/cm^2) for 24 h. The cells were then lysed, and the supernatants were subjected to luciferase and β-gal activity assay. Relative luciferase activity was determined by the ratio of luc to β-gal activity and normalized to that of the control. *Asterisk* indicates that the value was significantly different when compared to that of the control ($P<0.05$). **b** BEAS-2B cells were co-transfected with β-gal and NF-κB reporter plasmids and treated as above. Relative luciferase activity was analyzed. *Asterisk* indicates that the value was significantly different when compared to that of the control ($P<0.05$). **c** BEAS-2B cells were co-transfected with β-gal and VEGF reporter plasmids and treated as above. Relative luciferase activity was tested. *Asterisk* indicates that the value was significantly different when compared to that of the control ($P<0.05$)

WC-Co Nanoparticles Activated AKT and ERK1/2 Pathways Through ROS Generation

AKT and ERK are important signaling molecules in regulating multiple cellular functions. To determine whether WC-Co nanoparticles affect AKT and ERK activation, BEAS-2B cells were treated with the nano- or fine-sized WC-Co particles. The activation of AKT and ERK1/2 was analyzed by Western blotting. The nanoparticles were found to induce AKT and ERK1/2 activation at the low concentration of 2.5 μg/cm^2, while fine particles of WC-Co had only modest effect even at high concentrations (Fig. 3a). To test whether AKT or ERK1/2 activation was required for nanoparticle-induced ROS production, the cells were pretreated with a PI3K inhibitor (LY294002), an ERK 1/2inhibitor (U0126), or a H_2O_2 scavenger (catalase). When compared to the control, catalase treatment inhibited ROS production, but LY294002

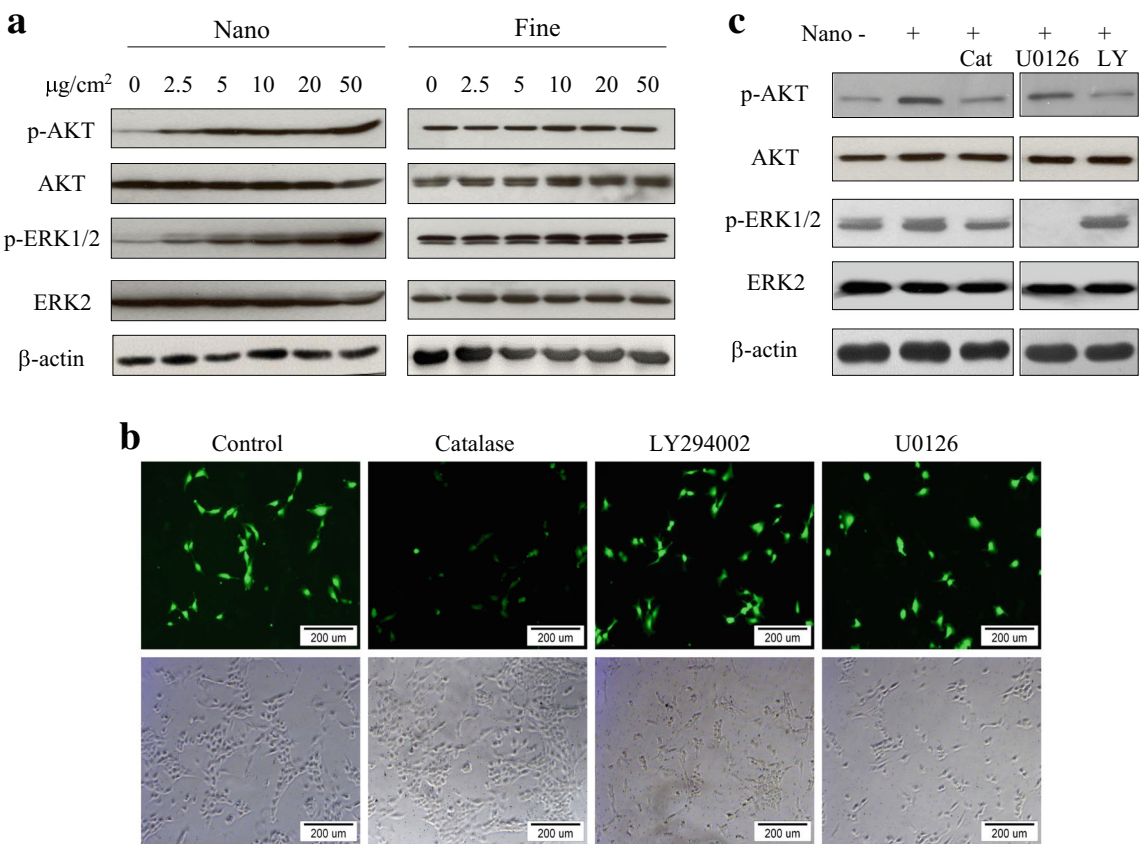

Fig. 3 Nanoparticles of WC-Co induced the activation of AKT and ERK1/2 pathways through ROS generation. **a** BEAS-2B cells were cultured in serum-free medium for 24 h. Then, cells were treated with various concentrations of nano size or fine size WC-Co for 1 h. Various proteins were subjected to immunoblotting. **b** BEAS-2B cells were seeded onto coverslips in the 6-well plate and incubated at 37 °C for 24 h. The cells were cultured in serum-free medium without or with 2000 U/ml of catalase, 20 μM LY294002, or 10 μM U0126 for 30 min. Then, cells were treated with 5 μ g/cm^2 WC-Co for 30 min. DCFH-DA was added, and fluorescent images were obtained as above. **c** BEAS-2B cells were cultured to 80 % confluence, then treated with 3000 U/ml of catalase, 20 μM U0126, or 20 μM LY294002 for 30 min in fresh medium. Then nano-sized WC-Co at 5 μg/cm^2 was added for 1 h. Cell lysates were subjected to Western blotting

or U0126 treatment had no inhibitory effect on ROS generation (Fig. 3b), suggesting that AKT and ERK1/2 might not act as upstream signaling molecules to regulate ROS generation. To test whether ROS may be the upstream regulator of AKT and ERK, the cells treated as above were analyzed for the activation of AKT and ERK by immunoblotting. The treatment of catalase inhibited levels of both phospho-AKT and phospho-ERK1/2 in the cells (Fig. 3c). As a control, LY294002 and U0126 decreased WC-Co nanoparticle-inducing AKT and ERK activation, respectively. These results indicate that WC-Co nanoparticles regulate AKT and ERK1/2 pathways through ROS production.

WC-Co Nanoparticles Induced AP-1, NF-κB and VEGF Transcriptional Activation via ROS, AKT, and ERK Pathways

To test whether transcriptional activation of AP-1, NF-κB, and VEGF is mediated through ROS production, or AKT and ERK1/2 activation, BEAS-2B cells were infected by adenovirus carrying catalase (Ad-cat), or treated by LY294002 and U0126, followed by the treatment with WC-Co nanoparticles. As shown in Fig. 4a–c, U0126 and LY294002 treatment decreased AP-1, NF-κB, and VEGF luciferase activity by more than 50 %. Inhibition of ROS production by catalase also significantly inhibited the transcriptional activation of AP-1, NF-κB, and VEGF. These results suggest that WC-Co nanoparticles induce ROS generation, activate AKT and ERK1/2 signaling pathways, which in turn regulate AP-1, NF-κB, and VEGF transcriptional activation.

The Treatment of BEAS-2B and A549 Cells with WC-Co Nanoparticles Induced Angiogenesis

Angiogenesis is an essential process during injury repair, inflammatory diseases, carcinogenesis, tumor growth, and metastasis [28]. To test the effect of WC-Co nanoparticles in angiogenesis, human lung epithelial BEAS-2B cells were treated without or with the nanoparticles at 5 μg/cm^2 for

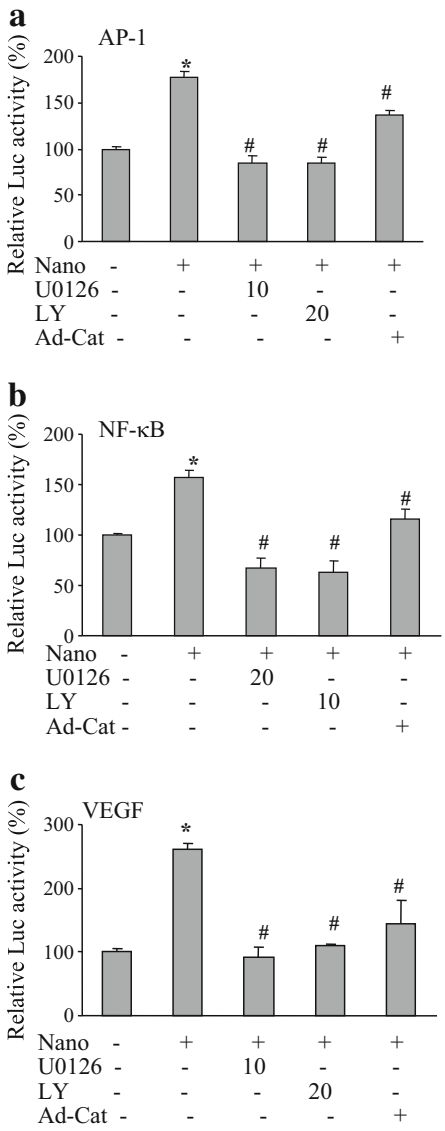

Fig. 4 Inhibition of ROS production, AKT, or ERK1/2 pathways decreased WC-Co nanoparticle-induced AP-1, NF-κB, and VEGF transcriptional activation. **a** BEAS-2B cells were co-transfected with AP-1 reporter and β-gal plasmids as Fig. 2c. Then cells were infected with or without adenovirus carrying GFP (Ad-GFP) or catalase (Ad-Cat) at 50 MOI for 24 h. Some cells were pretreated with 10 μM U0126 or 20 μM LY294002 for 30 min, and nano-sized WC-Co at 5 μg/cm^2 was added for 24 h. Luciferase assay was performed as above. **b** After co-transfection with NF-κB reporter and β-gal plasmids, BEAS-2B cells were infected with Ad-GFP or Ad-Cat as above or treated with 20 μM U0126 or 10 μM LY294002 for 30 min, then nanoparticles were added. Luciferase assay was performed. **c** After co-transfection with VEGF reporter and β-gal plasmids, BEAS-2B cells were infected with Ad-GFP or Ad-Cat, 10 μM U0126 or 20 μM LY294002 for 30 min, nano-sized WC-Co at 5 μg/cm^2 was added for 24 h. Luciferase assay was performed as in Fig. 2C. *Asterisk* indicates that the value was significantly different when compared to that of the control ($P<0.05$). *Number sign* indicates that the value was significantly different when compared to that of the nanoparticle treatment ($P<0.05$)

24 h. Then, the cells were used to perform an angiogenesis assay on the CAM. BEAS-2B cells alone did not increase angiogenesis, while the nanoparticle treatment greatly induced angiogenesis (Fig. 5a). The relative angiogenesis responses were analyzed by the number of microvessel branches in the unit area. The nanoparticle treatment increased the angiogenic response by more than fivefold when compared to the control group (Fig. 5b). To further test the effect of the nanoparticles on a different cell line, human lung adenocarcinoma cells A549 were treated as above to analyze the angiogenic response. Although A549 cells alone induced angiogenesis when compared to that of the Matrigel alone due to their tumor characteristic, treatment of the nanoparticles greatly enhanced the angiogenic response by fivefold when compared to that with A549 cells alone (Fig. 5c, d). These data indicate that the nanoparticles can stimulate different cells to induce angiogenesis. We also tested the effects of fine size particles on angiogenesis and found that the fine size particles at the same dose did not induce angiogenesis (data not shown).

Discussion

WC-Co is widely used as cemented carbide hard metals in a wide range of products in aerospace, automobiles, to home appliances. In contrast to hard metals, conventional materials have hardness and toughness which are mutually exclusive. WC-Co nanoparticles have many advantages over fine particles including the greatly improved toughness, hardness, and wear resistance. Occupational exposure to WC-Co has been associated with an increased risk of lung diseases including lung cancer [16, 17, 29, 30]. Previous studies have shown that WC-Co treatment induces micronuclei formation in rat lung [31]. During various processes, workers are exposed to various sizes of WC-Co particles including nanoparticles [32]. Recent evidence indicates that nanoparticles exhibit a higher deposition in all regions of the respiratory tract when compared to the fine particles, and that exposure to nanoparticles may induce cytotoxicity, pulmonary inflammation, and/or other adverse effects in the cells and lung [3]. However, the molecular mechanisms by which WC-Co exposure causes lung injury and carcinogenesis remain to be clarified. In this study, we found that WC-Co nanoparticles increase ROS production in the cells which induces other cellular signaling molecules.

AP-1 and NF-κB are important transcription factors involved in lung injury and inflammation [33–36]. VEGF is a potent angiogenic inducer [37, 38]. To study the molecular mechanism of WC-Co nanoparticles in inducing biologic effects, we found that low doses of WC-Co nanoparticles increased the transcriptional activation of AP-1, NF-κB, and VEGF (Fig. 6). These results are consistent with the nanoparticles increasing oxidative stress and generation of ROS. ROS are produced by all aerobic organisms through the oxygen reduction processor and can be induced by growth factors

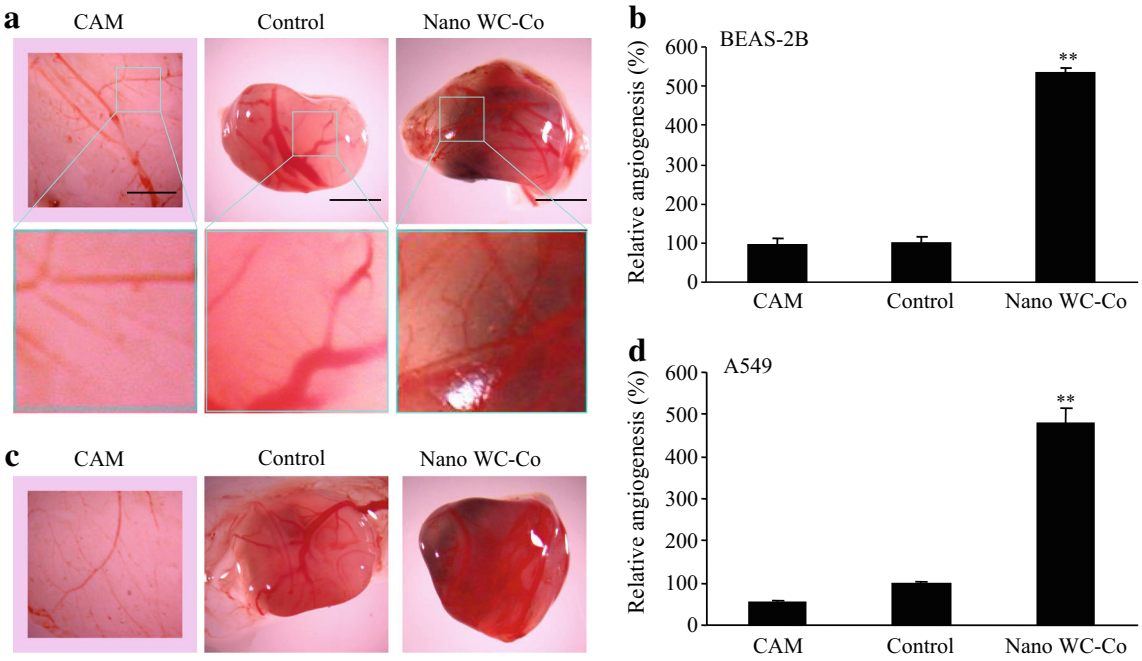

Fig. 5 BEAS-2B and A549 cells treated with nanoparticles of WC-Co induced angiogenesis in the chicken chorioallantoic membrane (CAM) model. **a** BEAS-2B cells were treated without or with 5 μg/cm^2 of nano WC-Co for 24 h, then trypsinized, resuspended in serum-free medium (3×10^7/ml, 0.1 ml), and mixed in 1:1 ratio with Matrigel (Collaborative Biomedical Products, Bedford, MA). Aliquots of the mixture were then applied to the CAM of 9-day-old embryos. After 96-h incubation, the area around the implanted Matrigel was photographed with a Nikon digital camera, and the numbers of newly formed vessels were counted. Assays for each treatment were carried out using 10 embryos per experiment. Representative photos generated from CAM alone or BEAS-2B cells treated without or with WC-Co (*upper panel*—low magnification; *bottom panel*—higher magnification). *Bar*: 2 mm. **b** The number of blood vessels was obtained by counting the branching of blood vessels and normalizing to the control (without WC-Co nanoparticles treatment) as relative angiogenesis. The data represent the mean±SD of the relative angiogenesis from 8 different embryos. *Asterisks* indicate that the value was significantly different when compared to that of the control ($P<0.01$). **c** Representative photos generated from CAM alone or A549 cells treated without or with WC-Co. Similar experiment was taken by using A549 cells, and angiogenesis was assayed as above. **d** Relative angiogenesis induced by A549 cells treated with WC-Co nanoparticles

and cytokines [23, 39]. Our results showed that nanoparticles, but not fine particles of WC-Co at 5 μg/cm^2 stimulate ROS production. As we expected, catalase inhibited ROS production, indicating that H_2O_2 is one of the species of ROS induced by nano-sized WC-Co. Growing evidence has shown that H_2O_2 may act as a second messenger to regulate various cellular functions and signaling pathways including ERK, phosphatidylinositol 3-kinase (PI3K), small GTPases, NF-κB, and nitrogen oxide (NO) pathways [40–44]. Previous reports indicate that PI3K and ERK may regulate ROS production [45, 46]. We found that the inhibitors of PI3K and ERK1/2, LY294002, and U0126 did not affect ROS generation. In contrast, treatment with catalase inhibited both AKT and ERK1/2. These results suggest that ROS act as upstream inducers of AKT and ERK1/2 in the cells. This finding is consistent with previous studies in a different cell system showing that H_2O_2 was the upstream regulator of AKT and ERK [47, 48]. We further showed that ROS, AKT, and ERK1/2 are upstream regulators of WC-Co nanoparticle-induced AP-1, NF-κB, and VEGF transcriptional activation.

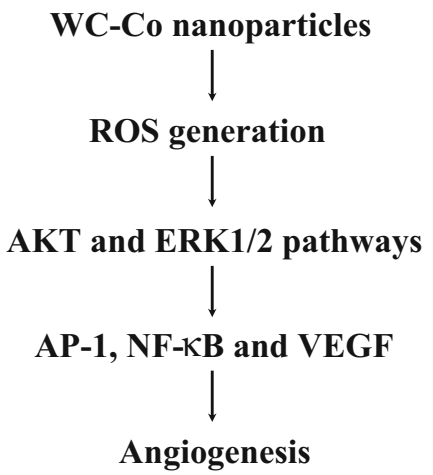

Fig. 6 The diagram summarizes our findings: WC-Co nanoparticles lead to ROS generation, which activates AKT and ERK1/2 pathways to induce angiogenesis via AP-1, NF-κB, and VEGF

Angiogenesis is critical in the injury repair, inflammation, tumor development, and neovascularization [49, 50]. Given the role of AP-1, NF-κB, and VEGF in regulating angiogenesis, to determine whether WC-Co nanoparticles can induce angiogenesis, we demonstrated that treatment of BEAS-2 cells with WC-Co nanoparticles at low dose induced angiogenesis, while equal dose of fine-sized WC-Co did not have a strong effect on angiogenesis. Similar results were obtained using

A549 cells, indicating that WC-Co nanoparticles enhanced A549 cells-induced angiogenesis. These results are consistent with the induction of transcriptional activation of AP-1, NF-κB, and VEGF in this study. These data elucidate cellular effects of WC-Co nanoparticles and potential molecular mechanisms involved in the response to WC-Co nanoparticle exposure.

Since more and more nanotechnologies are developed and various sizes of WC-Co were produced during the process of generating the hard metal, it is important to understand the biological effect of nanoparticles of WC-Co on inducing human diseases such as lung cancer, chronic pulmonary obstructive diseases, and bronchitis. Angiogenesis is well known to be closely associated with carcinogenesis, inflammatory diseases, and chronic pulmonary diseases including bronchitis. In this study, we found that nanoparticles of WC-Co induced ROS generation then increased the transcriptional activities of AP-1, NF-κB, and VEGF through activating AKT and ERK1/2 pathways, thus inducing angiogenesis. This study will afford useful information for preventing potential damage from nanoparticle exposure in the future.

Conclusions

These results illustrate that exposure to WC-Co nanoparticles induces angiogenic response by activating ROS, AKT, and ERK1/2 signaling pathways and the downstream molecules, including AP-1, NF-κB, and VEGF. This information may be useful for preventing potential damage from nanoparticle exposure in the future.

Acknowledgments This work was supported by R01HL091456, R01ES020868, and R21CA175975 from National Institutes of Health.

References

1. Roco MC (2004) Science and technology integration for increased human potential and societal outcomes. Ann N Y Acad Sci 1013:1–16
2. Renwick LC, Brown D, Clouter A, Donaldson K (2004) Increased inflammation and altered macrophage chemotactic responses caused by two ultrafine particle types. Occup Environ Med 61: 442–447
3. Gradon L, Orlicki D, Podgorski A (2000) Deposition and retention of ultrafine aerosol particles in the human respiratory system. Normal and pathological cases. Int J Occup Saf Ergon 6:189–207
4. Inoue K, Takano H, Yanagisawa R, Hirano S, Sakurai M, Shimada A, Yoshikawa T (2006) Effects of airway exposure to nanoparticles on lung inflammation induced by bacterial endotoxin in mice. Environ Health Perspect 114:1325–1330
5. Roberts RA, Shen T, Allen IC, Hasan W, DeSimone JM, Ting JP (2013) Analysis of the murine immune response to pulmonary delivery of precisely fabricated nano- and microscale particles. PLoS One 8:e62115
6. Oberdorster G, Ferin J, Lehnert BE (1994) Correlation between particle size, in vivo particle persistence, and lung injury. Environ Health Perspect 102(Suppl 5):173–179
7. Tanaka T, Kojima I, Ohse T, Ingelfinger JR, Adler S, Fujita T, Nangaku M (2005) Cobalt promotes angiogenesis via hypoxia-inducible factor and protects tubulointerstitium in the remnant kidney model. Lab Invest 85:1292–1307
8. Moulin JJ, Wild P, Romazini S, Lasfargues G, Peltier A, Bozec C, Deguerry P, Pellet F, Pedrix A (1998) Lung cancer risk in hard-metal workers. Am J Epidemiol 148:241–248
9. Lison D, Carbonnelle P, Mollo L, Lauwerys R, Fubini B (1995) Physicochemical mechanism of the interaction between cobalt metal and carbide particles to generate toxic activated oxygen species. Chem Res Toxicol 8:600–606
10. Wild P, Perdrix A, Romazini S, Moulin JJ, Pellet F (2000) Lung cancer mortality in a site producing hard metals. Occup Environ Med 57:568–573
11. Rinna A, Magdolenova Z, Hudecova A, Kruszewski M, Refsnes M, Dusinska M (2015) Effect of silver nanoparticles on mitogen-activated protein kinases activation: role of reactive oxygen species and implication in DNA damage. Mutagenesis 30:59–66
12. Durga M, Nathiya S, Rajasekar A, Devasena T (2014) Effects of ultrafine petrol exhaust particles on cytotoxicity, oxidative stress generation, DNA damage and inflammation in human A549 lung cells and murine RAW 264.7 macrophages. Environ Toxicol Pharmacol 38:518–530
13. Nakamura Y, Nishizaka Y, Ariyasu R, Okamoto N, Yoshida M, Taki M, Nagano H, Hanaoka K, Nakagawa K, Yoshimura C, Wakayama T, Amitani R (2014) Hard metal lung disease diagnosed on a transbronchial lung biopsy following recurrent contact dermatitis. Intern Med 53:139–143
14. Kaneko Y, Kikuchi N, Ishii Y, Kawabata Y, Moriyama H, Terada M, Suzuki E, Kobayashi M, Watanabe K, Hizawa N (2010) Upper lobe-dominant pulmonary fibrosis showing deposits of hard metal component in the fibrotic lesions. Intern Med 49:2143–2145
15. Tanaka J, Moriyama H, Terada M, Takada T, Suzuki E, Narita I, Kawabata Y, Yamaguchi T, Hebisawa A, Sakai F, Arakawa H (2014) An observational study of giant cell interstitial pneumonia and lung fibrosis in hard metal lung disease. BMJ Open 4:e004407
16. Wild P, Bourgkard E, Paris C (2009) Lung cancer and exposure to metals: the epidemiological evidence. Methods Mol Biol 472:139–167
17. Armstead AL, Arena CB, Li B (2014) Exploring the potential role of tungsten carbide cobalt (WC-Co) nanoparticle internalization in observed toxicity toward lung epithelial cells in vitro. Toxicol Appl Pharmacol 278:1–8
18. Jiang BH, Zheng JZ, Aoki M, Vogt PK (2000) Phosphatidylinositol 3-kinase signaling mediates angiogenesis and expression of vascular endothelial growth factor in endothelial cells. Proc Natl Acad Sci U S A 97:1749–1753
19. He TC, Zhou S, da Costa LT, Yu J, Kinzler KW, Vogelstein B (1998) A simplified system for generating recombinant adenoviruses. Proc Natl Acad Sci U S A 95:2509–2514
20. Bauer G (2000) Reactive oxygen and nitrogen species: efficient, selective, and interactive signals during intercellular induction of apoptosis. Anticancer Res 20:4115–4139
21. Forman HJ, Fukuto JM, Torres M (2004) Redox signaling: thiol chemistry defines which reactive oxygen and nitrogen species can act as second messengers. Am J Physiol Cell Physiol 287:C246–C256
22. Schieber M, Chandel NS (2014) ROS function in redox signaling and oxidative stress. Curr Biol 24:R453–R462
23. Liu LZ, Hu XW, Xia C, He J, Zhou Q, Shi X, Fang J, Jiang BH (2006) Reactive oxygen species regulate epidermal growth factor-induced vascular endothelial growth factor and hypoxia-inducible

factor-1alpha expression through activation of AKT and P70S6K1 in human ovarian cancer cells. Free Radic Biol Med 41:1521–1533
24. Carpenter RL, Jiang Y, Jing Y, He J, Rojanasakul Y, Liu LZ, Jiang BH (2011) Arsenite induces cell transformation by reactive oxygen species, AKT, ERK1/2, and p70S6K1. Biochem Biophys Res Commun 414:533–538
25. Hsu TC, Young MR, Cmarik J, Colburn NH (2000) Activator protein 1 (AP-1)- and nuclear factor kappaB (NF-kappaB)-dependent transcriptional events in carcinogenesis. Free Radic Biol Med 28: 1338–1348
26. Manduteanu I, Dragomir E, Voinea M, Capraru M, Simionescu M (2007) Enoxaparin reduces H2O2-induced activation of human endothelial cells by a mechanism involving cell adhesion molecules and nuclear transcription factors. Pharmacology 79:154–162
27. Zhou Q, Liu LZ, Fu B, Hu X, Shi X, Fang J, Jiang BH (2007) Reactive oxygen species regulate insulin-induced VEGF and HIF-1alpha expression through the activation of p70S6K1 in human prostate cancer cells. Carcinogenesis 28:28–37
28. Folkman J (1974) Tumor angiogenesis. Adv Cancer Res 19:331–358
29. Armstead AL, Minarchick VC, Porter DW, Nurkiewicz TR, Li B (2015) Acute inflammatory responses of nanoparticles in an intratracheal instillation rat model. PLoS One 10, e0118778
30. Dunlop P, Muller NL, Wilson J, Flint J, Churg A (2005) Hard metal lung disease: high resolution CT and histologic correlation of the initial findings and demonstration of interval improvement. J Thorac Imaging 20:301–304
31. De Boeck M, Hoet P, Lombaert N, Nemery B, Kirsch-Volders M, Lison D (2003) In vivo genotoxicity of hard metal dust: induction of micronuclei in rat type II epithelial lung cells. Carcinogenesis 24: 1793–1800
32. Stefaniak AB, Virji MA, Day GA (2009) Characterization of exposures among cemented tungsten carbide workers. Part I: size-fractionated exposures to airborne cobalt and tungsten particles. J Expo Sci Environ Epidemiol 19:475–491
33. Alvira CM (2014) Nuclear factor-kappa-B signaling in lung development and disease: one pathway, numerous functions. Birth Defects Res A Clin Mol Teratol 100:202–216
34. Chopra M, Reuben JS, Sharma AC (2009) Acute lung injury: apoptosis and signaling mechanisms. Exp Biol Med (Maywood) 234: 361–371
35. Lee IT, Yang CM (2013) Inflammatory signalings involved in airway and pulmonary diseases. Mediators Inflamm 2013:791231
36. Verstrepen L, Beyaert R (2014) Receptor proximal kinases in NF-kappaB signaling as potential therapeutic targets in cancer and inflammation. Biochem Pharmacol 92:519–529
37. Shibuya M (2015) VEGF-VEGFR system as a target for suppressing inflammation and other diseases. Endocr Metab Immune Disord Drug Targets
38. Connolly DT, Heuvelman DM, Nelson R, Olander JV, Eppley BL, Delfino JJ, Siegel NR, Leimgruber RM, Feder J (1989) Tumor vascular permeability factor stimulates endothelial cell growth and angiogenesis. J Clin Invest 84:1470–1478
39. Yang L, Liu G, Lin Z, Wang Y, He H, Liu T, Kamp DW (2014) Pro-inflammatory response and oxidative stress induced by specific components in ambient particulate matter in human bronchial epithelial cells. Environ Toxicol
40. Bae YS, Sung JY, Kim OS, Kim YJ, Hur KC, Kazlauskas A, Rhee SG (2000) Platelet-derived growth factor-induced H (2) O (2) production requires the activation of phosphatidylinositol 3-kinase. J Biol Chem 275:10527–10531
41. Finkel T (1998) Oxygen radicals and signaling. Curr Opin Cell Biol 10:248–253
42. May JM, de Haen C (1979) The insulin-like effect of hydrogen peroxide on pathways of lipid synthesis in rat adipocytes. J Biol Chem 254:9017–9021
43. Schreck R, Albermann K, Baeuerle PA (1992) Nuclear factor kappa B: an oxidative stress-responsive transcription factor of eukaryotic cells (a review). Free Radic Res Commun 17:221–237
44. Vercellotti GM, Severson SP, Duane P, Moldow CF (1991) Hydrogen peroxide alters signal transduction in human endothelial cells. J Lab Clin Med 117:15–24
45. Baumer AT, Ten Freyhaus H, Sauer H, Wartenberg M, Kappert K, Schnabel P, Konkol C, Hescheler J, Vantler M, Rosenkranz S (2008) Phosphatidylinositol 3-kinase-dependent membrane recruitment of Rac-1 and p47phox is critical for alpha-platelet-derived growth factor receptor-induced production of reactive oxygen species. J Biol Chem 283:7864–7876
46. Zhuang S, Kinsey G, Yan Y, Han J, Schnellmann R (2008) ERK activation mediates mitochondrial dysfunction and necrosis induced by hydrogen peroxide in renal proximal tubular cells. J Pharmacol Exp Ther 325:732–740
47. Tournier C, Thomas G, Pierre J, Jacquemin C, Pierre M, Saunier B (1997) Mediation by arachidonic acid metabolites of the H2O2-induced stimulation of mitogen-activated protein kinases (extracellular-signal-regulated kinase and c-Jun NH2-terminal kinase). Eur J Biochem 244:587–595
48. Ushio-Fukai M, Alexander RW, Akers M, Yin Q, Fujio Y, Walsh K, Griendling KK (1999) Reactive oxygen species mediate the activation of Akt/protein kinase B by angiotensin II in vascular smooth muscle cells. J Biol Chem 274:22699–22704
49. Folkman J (1995) Angiogenesis in cancer, vascular, rheumatoid and other disease. Nat Med 1:27–31
50. Risau W (1997) Mechanisms of angiogenesis. Nature 386:671–674